

## Research Article

# Growth and Mechanism of MoS<sub>2</sub> Nanoflowers with Ultrathin Nanosheets

Yifei Guo,<sup>1,2</sup> Xiuli Fu,<sup>1</sup> and Zhijian Peng<sup>2</sup>

<sup>1</sup>State Key Laboratory of Information Photonics and Optical Communications and School of Science, Beijing University of Posts and Telecommunications, Beijing 100876, China

<sup>2</sup>School of Engineering and Technology, China University of Geosciences, Beijing 100083, China

Correspondence should be addressed to Xiuli Fu; [xiulifu@bupt.edu.cn](mailto:xiulifu@bupt.edu.cn) and Zhijian Peng; [pengzhijian@cugb.edu.cn](mailto:pengzhijian@cugb.edu.cn)

Received 26 October 2016; Accepted 14 February 2017; Published 19 March 2017

Academic Editor: Jean M. Greneche

Copyright © 2017 Yifei Guo et al. This is an open access article distributed under the Creative Commons Attribution License, which permits unrestricted use, distribution, and reproduction in any medium, provided the original work is properly cited.

Two-dimensional molybdenum disulfide (MoS<sub>2</sub>) with few layers, due to their excellent optical and electrical properties, has great potential for applications in electronic and optoelectronic devices. In this work, flower-like MoS<sub>2</sub> nanostructures with ultrathin nanosheets (petals) were successfully deposited onto silicon substrates by a facile process based on chemical vapor deposition via using MoO<sub>3</sub> and S powders as starting materials. Their composition and structure were explored by field emission scanning electron microscopy, transmission electron microscopy, Raman spectroscopy, and photoluminescence. The reported nanoflowers vertically and separately stood on the substrates, consisting of several bonded MoS<sub>2</sub> nanosheets with a thickness of 10–30 nm and high crystallinity. On the basis of these results, a growth mechanism for the MoS<sub>2</sub> nanoflowers was proposed.

## 1. Introduction

Over the past decades, two-dimensional semiconducting transition metal dichalcogenides (TMDs) have received extensive attention because of their unique structure as well as excellent optical and electrical properties [1–4]. Recently, some authors have reported the exciting applications of TMDs (such as MoS<sub>2</sub>, WS<sub>2</sub>, MoSe<sub>2</sub>, and WSe<sub>2</sub>) in photovoltaics [5], energy storage [6], photocatalysts [7], and optoelectronic devices [8, 9]. Among them, MoS<sub>2</sub> exhibits novel properties because of its unique atomic structure. MoS<sub>2</sub> is composed of three atomic layers: the molybdenum atoms layer sandwiched between two layers of sulfur atoms. There are strong covalent bonds within the layers and weak van der Waals force between the lattice layers. So far, various morphologies of MoS<sub>2</sub> have been reported, including nanoplates [10, 11], nanorods [12], nanowires [13], nanotubes [14], and nanoflowers [15]. In addition, more recent studies have revealed that three-dimensional MoS<sub>2</sub> structures are much more desirable in many specific applications because of their remarkable advantages, such as more actively exposed edges and high aspect ratio [16, 17]. For

instance, the exposed edges may play a crucial role in electrochemical and catalytic reactions due to the active dangling bonds.

With regard to the synthesis of MoS<sub>2</sub>, several groups have prepared MoS<sub>2</sub> by a variety of methods, including mechanical exfoliation [18], lithium-based intercalation [19, 20], hydrothermal synthesis [21, 22], chemical vapor transport [23], and chemical vapor deposition (CVD) [24, 25]. To date, three-dimensional MoS<sub>2</sub> nanostructures, such as nanoflowers and nanospheres, are obtained mainly by hydrothermal synthesis [26, 27]. Compared to hydrothermal synthesis, CVD, a typical bottom-up growth method, has several advantages, such as being more facile, having a lower cost, and causing less pollution, presenting great potential as an efficient technique towards scalable synthesis of high-quality MoS<sub>2</sub>. However, there are very few studies on the growth of MoS<sub>2</sub> nanoflowers by CVD methods [28, 29]. So, in this work, we designed a facile process based on CVD, which can obtain a kind of flower-like MoS<sub>2</sub> nanostructures with ultrathin nanosheets (petals). And the growth mechanism of the reported MoS<sub>2</sub> nanoflowers was proposed.

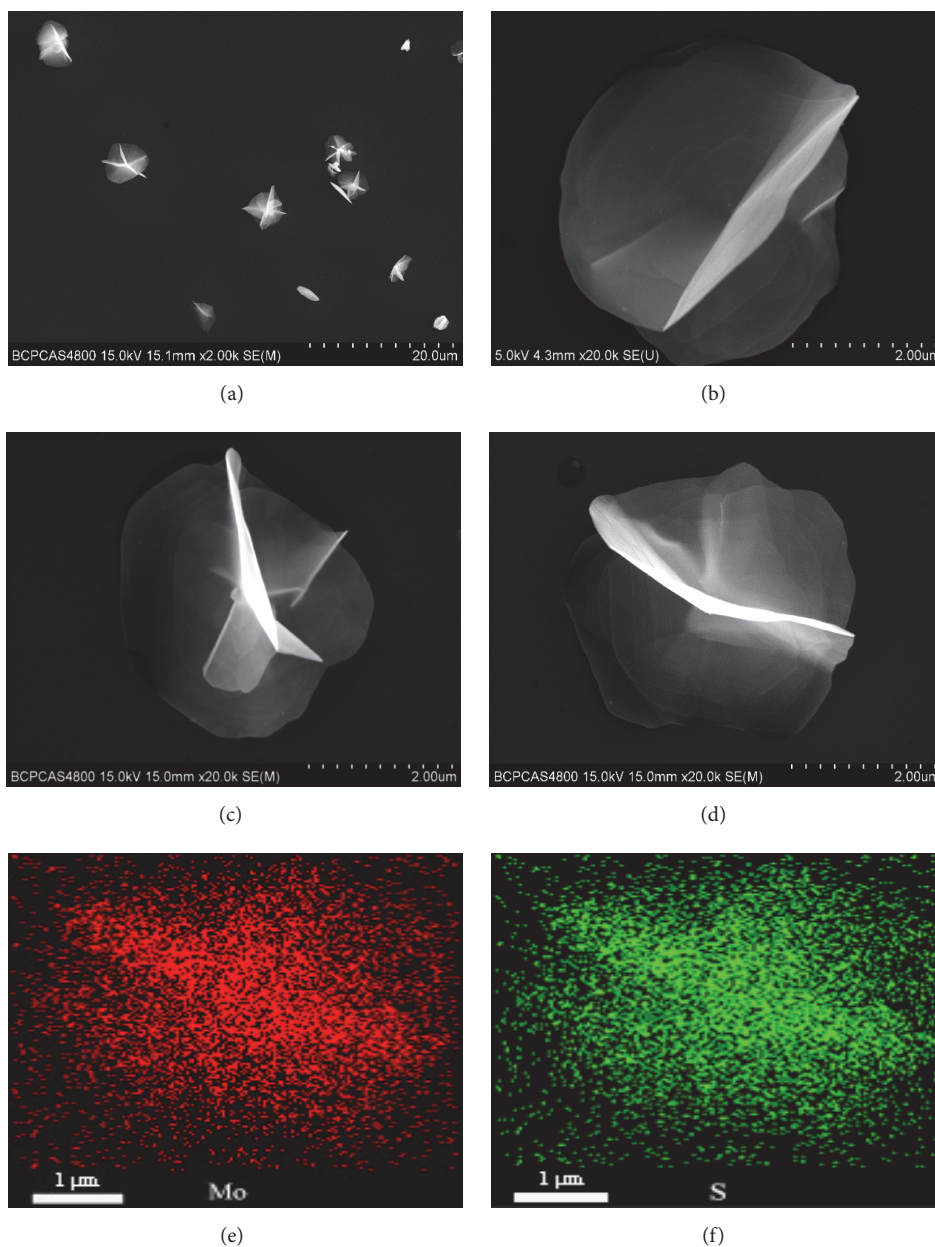


FIGURE 1: Typical SEM images of the obtained samples in low magnification (a) and high magnification (b, c, d). (e, f) EDX mapping results on one sheet of the sample.

## 2. Experimental

The as-proposed vertically grown  $\text{MoS}_2$  nanoflowers with ultrathin nanosheets were prepared by CVD in a horizontal quartz tube furnace with two temperature zones working with different heating resistors [30]. By making use of this equipment, we can effectively and accurately control the temperature gradient of the furnace along the quartz tube. In a typical process, pure  $\text{MoO}_3$  and S powders as starting materials were loaded in two different alumina boats. The boat with  $\text{MoO}_3$  powder was placed at the center of the high-temperature zone, and that with S powder was located

at 12 cm away from the  $\text{MoO}_3$  powder on the upstream of the carrier gas in the furnace. Meanwhile, by placing on a quartz plate, a Si wafer was set on the carrier gas downstream of the furnace at the center of the low-temperature zone, which was about 60 cm apart from the evaporation source  $\text{MoO}_3$  powder. Before heating, the tube furnace was first evacuated and flushed repeatedly with Ar gas several times to deplete the remnant oxygen in the whole system. Subsequently, the high-temperature zone was ramped up to  $850^\circ\text{C}$  in 40 min and then held at  $850^\circ\text{C}$  for 1 h, while the low-temperature zone was heated up to  $500^\circ\text{C}$  in 30 min and held at  $500^\circ\text{C}$  for 70 min. After heating, the furnace was

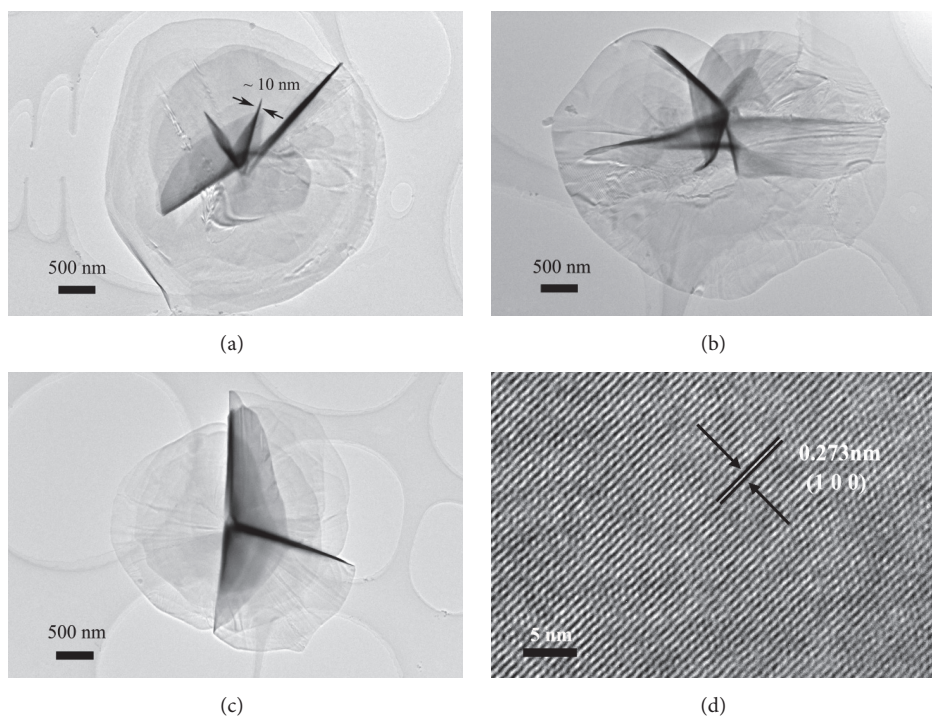


FIGURE 2: (a, b, c) TEM images of the obtained flower-like MoS<sub>2</sub> nanostructures. (d) HRTEM image of typical MoS<sub>2</sub> nanosheet.

cooled naturally to room temperature. Throughout the whole reaction process, an Ar gas flow of 200 sccm was kept inside the quartz tube. Finally, the samples were collected on the Si wafer.

The morphology and structure of the as-synthesized samples were characterized by optical microscopy (OM, Olympus BX53), field emission scanning electron microscopy (SEM, S4800), transmission electron microscopy (TEM, Tecnai G2 F20 U-TWIN), and high-resolution transmission electron microscopy (HRTEM, Tecnai G2 F20 U-TWIN). An energy-dispersive X-ray (EDX) spectroscope attached to the SEM was used to measure the composition of the samples. The optical properties and quality of the as-grown samples were examined by Raman spectroscopy and photoluminescence (PL), which were carried out on a Jobin Yvon HR800 Raman system with a laser excited at 532 nm. A laser power of 0.1 mW was used to avoid heating the sample and PL saturation.

### 3. Results and Discussion

The morphology of the as-prepared samples was first examined by SEM. Typical results are presented in Figure 1. The low magnification image as shown in Figure 1(a) displays a number of flower-like nanostructures, all of which stood on the substrate (Si wafer). For individual nanostructure, the high magnification images as shown in Figures 1(b)–1(d) indicate that although the morphology of the flowers might vary somewhat, all of them consist of several bonded ultrathin nanosheets (petals), which are of largely exposed surfaces (including side edges) and grow relatively independently

of each other. Notably, the petals of nanostructures display different curving angles and are of a diameter of roughly 4–6  $\mu\text{m}$ . Furthermore, the EDX mapping images of the sample (as shown in Figures 1(e) and 1(f)) reveal that the as-grown samples were molybdenum sulfide nanostructures, and the calculated atomic ratio of the samples is approximately Mo : S = 1 : 2.08, which is very much approaching the stoichiometric ratio of MoS<sub>2</sub>.

In order to elucidate the crystalline structure of the samples, TEM examinations were carried out. The characteristics of the present nanostructures with some thin petals could be also observed from the TEM images as illustrated in Figures 2(a)–2(c). Although the TEM samples were prepared by ultrasonic dispersion and transferred onto the supporting grid, the intact morphology of MoS<sub>2</sub> nanoflowers as shown in Figures 2(a)–2(c) indicates good structural stability and high crystallinity of the samples, confirming the flower-like nanostructure of the samples. Moreover, under the irradiation of electron beam, the nanosheets of the flower-like nanostructures were found to be very much transparent, revealing that they are ultrathin pieces. The size of the flower-like nanostructures was also evaluated by TEM (see Figure 2(a)). It was calculated that their diameter was in the range of roughly 4–6  $\mu\text{m}$ , which is consistent with the SEM observation, and the thickness of the nanosheets (petals) was in the range of approximately 10–30 nm. Moreover, a typical HRTEM image on a nanosheet of the obtained nanostructures was presented in Figure 2(d), showing that the lattice distance is 0.273 nm, corresponding to the (100) plane of the MoS<sub>2</sub> phase, which is consistent with the EDX results from SEM.



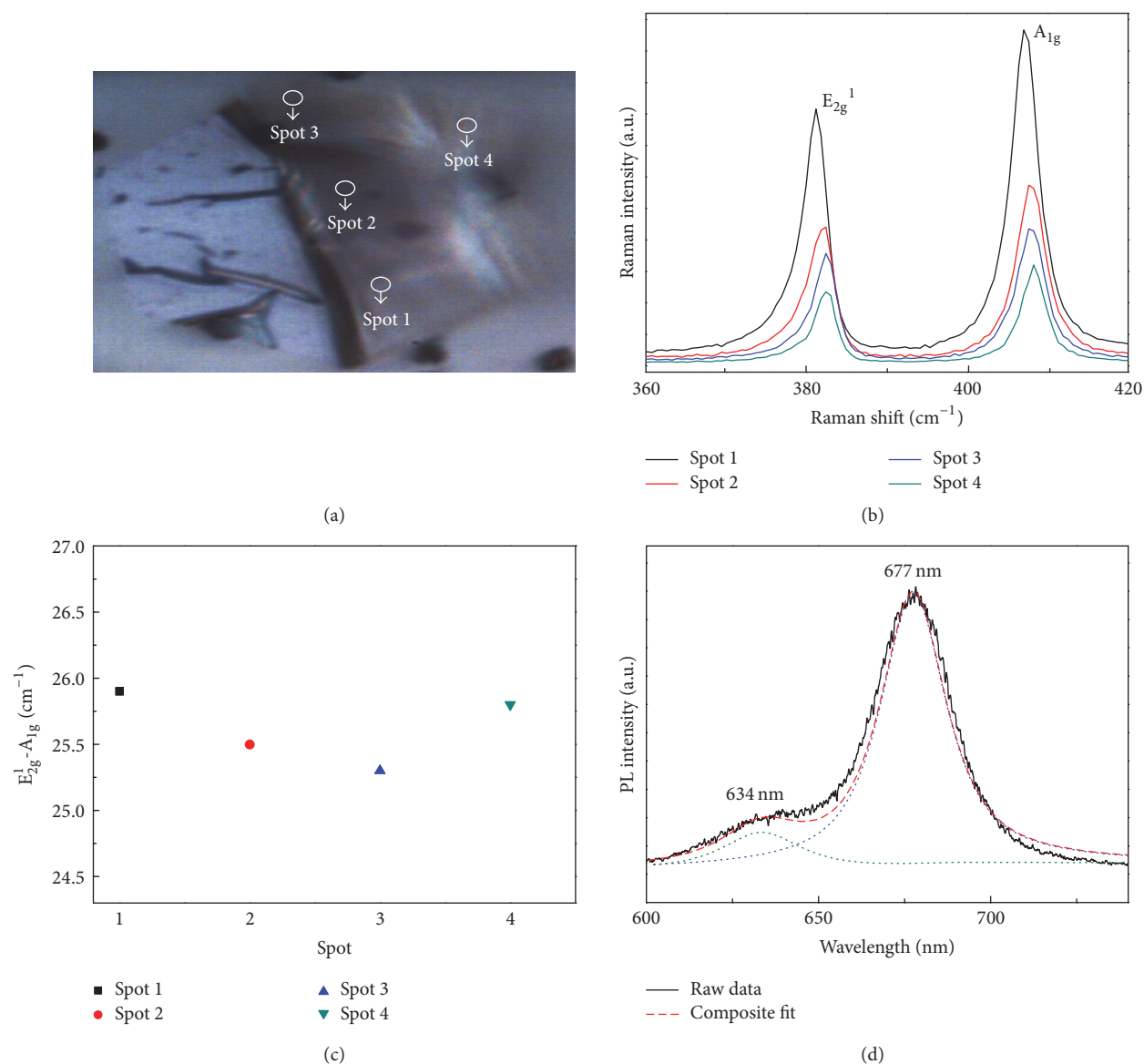


FIGURE 3: (a) OM image of a typical MoS<sub>2</sub> nanosheet, where the Raman spectra were recorded at different places, marked as Spots 1–4. (b) The recorded Raman patterns from the different spots on the MoS<sub>2</sub> nanosheet and (c) their corresponding differences between E<sub>2g</sub><sup>1</sup> and A<sub>1g</sub> modes. (d) Typical PL spectrum of a MoS<sub>2</sub> nanosheet.

To further investigate the optical properties and quality of the as-grown nanostructures with ultrathin MoS<sub>2</sub> nanosheets, Raman and PL measurements were performed. Figure 3(a) displays the OM image of a typical MoS<sub>2</sub> nanosheet, where the Raman spectra were recorded at different places marked as Spots 1–4 in the figure. The results are presented in Figure 3(b). As shown in Figure 3(b), two typical Raman active peaks of MoS<sub>2</sub>, in-plane vibration E<sub>2g</sub><sup>1</sup> and out-of-plane vibration A<sub>1g</sub>, are exhibited, which are located at about 381 and 407 cm<sup>-1</sup>, respectively. As is well known, the difference ( $\Delta$ ) between E<sub>2g</sub><sup>1</sup> and A<sub>1g</sub> modes can be used to estimate the thickness difference and layer number of MoS<sub>2</sub> nanosheets; and the  $\Delta$  value is about 20 cm<sup>-1</sup> for monolayer

and approximately 25 cm<sup>-1</sup> for multilayer MoS<sub>2</sub> [31]. From Figure 3(c), it can be seen that the calculated  $\Delta$  values from the different spots on a typical MoS<sub>2</sub> nanosheet fluctuate in a very narrow range of 25.3–25.9 cm<sup>-1</sup>, indicating that the nanosheets were multilayer MoS<sub>2</sub> and the thicknesses of the MoS<sub>2</sub> nanosheet are quite homogeneous. Moreover, the PL spectrum as shown in Figure 3(d) can be fitted into two prominent emission peaks at about 634 and 677 nm, which are, respectively, assigned to the A<sub>1</sub> excitation with a peak energy of about 1.96 eV and the resonance of B<sub>1</sub> excitation with a peak energy of approximately 1.83 eV. Additionally, due to the A<sub>1</sub> and B<sub>1</sub> direct excitonic transitions, the emissions could not found from their direct band-gap bulk materials. Therefore, the above Raman and PL

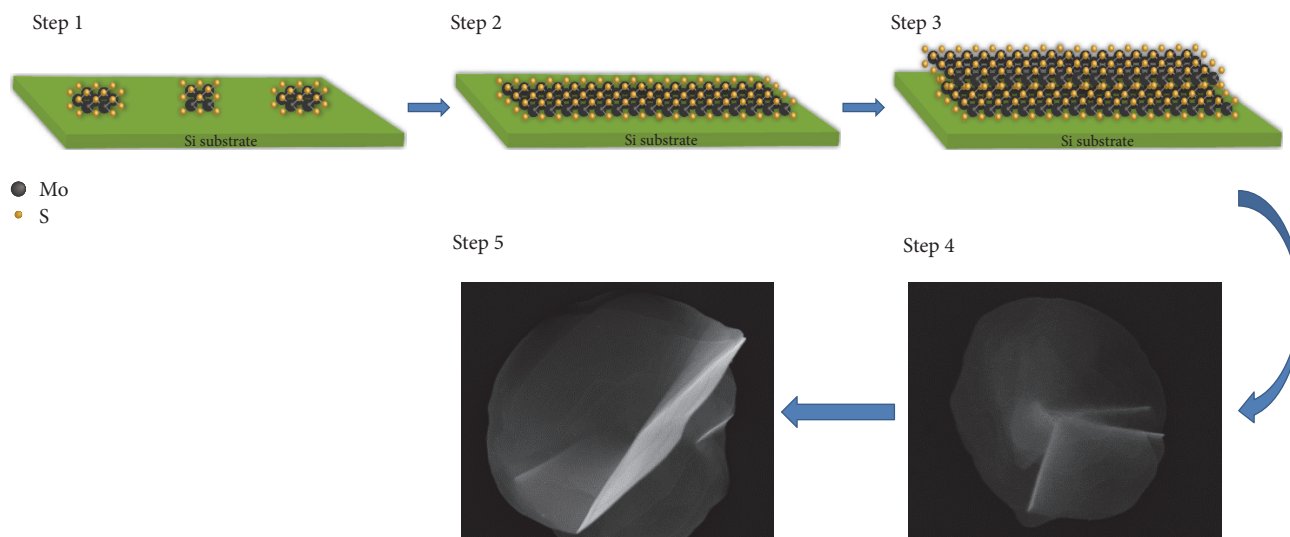


FIGURE 4: Schematic diagram for the growth mechanism of the flower-like MoS<sub>2</sub> nanostructures.

results qualitatively indicate that the obtained MoS<sub>2</sub> nanosheets are of few layers and could exhibit a very strong PL emission.

Finally, we try to propose a growth mechanism for the flower-like MoS<sub>2</sub> nanostructures. In the early stage of reactions, S vapor transported by the Ar carrier gas reacts with the MoO<sub>3</sub> powder, and the MoO<sub>3</sub> would be reduced gradually, forming gaseous MoS<sub>2</sub>, which will spread to the silicon substrate. The nucleation sites (crystal seeds) of MoS<sub>2</sub> thin films are subsequently formed (see Step 1 in Figure 4) [32]. As the growth proceeded, MoS<sub>2</sub> thin films were formed owing to the growth and merging of the crystal seeds (Step 2). With the growth continued, MoS<sub>2</sub> thin films firstly grew into a layer-by-layer pattern until a critical thickness reached, and then merged and extended constantly (Step 3). During the growth, due to possible dynamics cause and local heating, slight edge dislocation and little curve would be formed. Then, the curve direction gradually became energetically favorable, which led to the vertically grown MoS<sub>2</sub> nanosheets (Step 4). At last, MoS<sub>2</sub> films slipped and grew in a vertical pattern, forming the as-proposed MoS<sub>2</sub> nanoflowers (Step 5). And at the temperature holding stage, some amorphous and defect structures grew further, leading to the nanoflowers with high crystallinity. From our result, it can be inferred that the formation of the edge dislocations and curve may result in distinct morphologies of flower-like structures in several areas. Obviously, some petals grew gradually along the preferred curly growth direction, forming a number of single MoS<sub>2</sub> nanoflowers.

In addition, because many two-dimensional semiconducting TMDs have similar layered structure and physical property with MoS<sub>2</sub>, the above-observed edge dislocation and curve during their formation would usually occur [33, 34]. Therefore, under an appropriate condition on dynamics and local heating, the present CVD approach might be also used to grow flower-like or more complex structures of other two-dimensional layered materials, such as oxides, sulphides,

and selenides, by using their oxides and/or S/Se powders as the starting materials.

## 4. Conclusions

Flower-like MoS<sub>2</sub> nanostructures with ultrathin nanosheets (petals) were successfully synthesized by a facile CVD technique onto silicon substrates via using MoO<sub>3</sub> and S powders as starting materials. The vertically and separately standing nanoflowers consist of few layers of MoS<sub>2</sub> nanosheets with a thickness of 10–30 nm and have high crystallinity, which would be promising in the applications in nanoscaled electronic and optical devices. And the growth of MoS<sub>2</sub> nanoflowers is caused by the formation of edge dislocations and curve, which may be used in growing flower-like or more complex structures of other two-dimensional layered materials.

## Conflicts of Interest

The authors declare that there are no conflicts of interest regarding the publication of this paper.

## Acknowledgments

The authors would like to acknowledge the financial support for this work from the National Natural Science Foundation of China (Grants nos. 11674035, 61274015, and 11274052) and Fund of State Key Laboratory of Information Photonics and Optical Communications (Beijing University of Posts and Telecommunications).

## References

- [1] B. Radisavljevic, A. Radenovic, J. Brivio, V. Giacometti, and A. Kis, "Single-layer MoS<sub>2</sub> transistors," *Nature Nanotechnology*, vol. 6, no. 3, pp. 147–150, 2011.

- [2] Q. H. Wang, K. Kalantar-Zadeh, A. Kis, J. N. Coleman, and M. S. Strano, "Electronics and optoelectronics of two-dimensional transition metal dichalcogenides," *Nature Nanotechnology*, vol. 7, no. 11, pp. 699–712, 2012.
- [3] C. R. Dean, A. F. Young, I. Meric et al., "Boron nitride substrates for high-quality graphene electronics," *Nature Nanotechnology*, vol. 5, no. 10, pp. 722–726, 2010.
- [4] A. Hsu, H. Wang, Y. C. Shin et al., "Large-area 2-D electronics: materials, technology, and devices," *Proceedings of the IEEE*, vol. 101, no. 7, pp. 1638–1652, 2013.
- [5] S. Wi, H. Kim, M. Chen et al., "Enhancement of photovoltaic response in multilayer MoS<sub>2</sub> induced by plasma doping," *ACS Nano*, vol. 8, no. 5, pp. 5270–5281, 2014.
- [6] T. Stephenson, Z. Li, B. Olsen, and D. Mitlin, "Lithium ion battery applications of molybdenum disulfide (MoS<sub>2</sub>) nanocomposites," *Energy and Environmental Science*, vol. 7, no. 1, pp. 209–231, 2014.
- [7] B. Mahler, V. Hoepfner, K. Liao, and G. A. Ozin, "Colloidal synthesis of 1T-WS<sub>2</sub> and 2H-WS<sub>2</sub> nanosheets: applications for photocatalytic hydrogen evolution," *Journal of the American Chemical Society*, vol. 136, no. 40, pp. 14121–14127, 2014.
- [8] M. Amani, M. L. Chin, A. G. Birdwell et al., "Electrical performance of monolayer MoS<sub>2</sub> field-effect transistors prepared by chemical vapor deposition," *Applied Physics Letters*, vol. 102, no. 19, Article ID 193107, 2013.
- [9] R. S. Sundaram, M. Engel, A. Lombardo et al., "Electroluminescence in single layer MoS<sub>2</sub>," *Nano Letters*, vol. 13, no. 4, pp. 1416–1421, 2013.
- [10] Z. Wu, D. Wang, and A. Sun, "Preparation of MoS<sub>2</sub> nanoflakes by a novel mechanical activation method," *Journal of Crystal Growth*, vol. 312, no. 2, pp. 340–343, 2010.
- [11] Z. Wu, D. Wang, X. Liang, and A. Sun, "Novel hexagonal MoS<sub>2</sub> nanoplates formed by solid-state assembly of nanosheets," *Journal of Crystal Growth*, vol. 312, no. 12–13, pp. 1973–1976, 2010.
- [12] H. Lin, X. Chen, H. Li, M. Yang, and Y. Qi, "Hydrothermal synthesis and characterization of MoS<sub>2</sub> nanorods," *Materials Letters*, vol. 64, no. 15, pp. 1748–1750, 2010.
- [13] W.-J. Li, E.-W. Shi, J.-M. Ko, Z.-Z. Chen, H. Ogino, and T. Fukuda, "Hydrothermal synthesis of MoS<sub>2</sub> nanowires," *Journal of Crystal Growth*, vol. 250, no. 3–4, pp. 418–422, 2003.
- [14] J. Chen, S.-L. Li, Q. Xu, and K. Tanaka, "Synthesis of open-ended MoS<sub>2</sub> nanotubes and the application as the catalyst of methanation," *Chemical Communications*, no. 16, pp. 1722–1723, 2002.
- [15] G. Tang, J. Sun, C. Wei et al., "Synthesis and characterization of flowerlike MoS<sub>2</sub> nanostructures through CTAB-assisted hydrothermal process," *Materials Letters*, vol. 86, pp. 9–12, 2012.
- [16] T. Yang, Y. J. Chen, B. H. Qu et al., "Construction of 3D flower-like MoS<sub>2</sub> spheres with nanosheets as anode materials for high-performance lithium ion batteries," *Electrochimica Acta*, vol. 115, pp. 165–169, 2014.
- [17] X. Zhao, C. Hu, and M. Cao, "Three-dimensional MoS<sub>2</sub> hierarchical nanoarchitectures anchored into a carbon layer as graphene analogues with improved lithium ion storage performance," *Chemistry—An Asian Journal*, vol. 8, no. 11, pp. 2701–2707, 2013.
- [18] H. Li, G. Lu, Z. Yin et al., "Optical identification of single- and few-layer MoS<sub>2</sub> sheets," *Small*, vol. 8, no. 5, pp. 682–686, 2012.
- [19] P. Joensen, R. F. Frindt, and S. R. Morrison, "Single-layer MoS<sub>2</sub>," *Materials Research Bulletin*, vol. 21, no. 4, pp. 457–461, 1986.
- [20] A. Schumacher, L. Scandella, N. Kruse, and R. Prins, "Single-layer MoS<sub>2</sub> on mica: studies by means of scanning force microscopy," *Surface Science*, vol. 289, no. 1–2, pp. L595–L598, 1993.
- [21] X. Zhou, B. Xu, Z. Lin, D. Shu, and L. Ma, "Hydrothermal synthesis of flower-like MoS<sub>2</sub> nanospheres for electrochemical supercapacitors," *Journal of Nanoscience and Nanotechnology*, vol. 14, no. 9, pp. 7250–7254, 2014.
- [22] H. Yu, X. Yu, Y. Chen, S. Zhang, P. Gao, and C. Li, "A strategy to synergistically increase the number of active edge sites and the conductivity of MoS<sub>2</sub> nanosheets for hydrogen evolution," *Nanoscale*, vol. 7, no. 19, pp. 8731–8738, 2015.
- [23] A. Castellanos-Gomez, M. Barkelid, A. M. Goossens, V. E. Calado, H. S. J. Van Der Zant, and G. A. Steele, "Laser-thinning of MoS<sub>2</sub>: on demand generation of a single-layer semiconductor," *Nano Letters*, vol. 12, no. 6, pp. 3187–3192, 2012.
- [24] Y. Zhan, Z. Liu, S. Najmaei, P. M. Ajayan, and J. Lou, "Large-area vapor-phase growth and characterization of MoS<sub>2</sub> atomic layers on a SiO<sub>2</sub> substrate," *Small*, vol. 8, no. 7, pp. 966–971, 2012.
- [25] S. Balendhran, J. Z. Ou, M. Bhaskaran et al., "Atomically thin layers of MoS<sub>2</sub> via a two step thermal evaporation-exfoliation method," *Nanoscale*, vol. 4, no. 2, pp. 461–466, 2012.
- [26] B. Sheng, J. Liu, Z. Li et al., "Effects of excess sulfur source on the formation and photocatalytic properties of flower-like MoS<sub>2</sub> spheres by hydrothermal synthesis," *Materials Letters*, vol. 144, no. 9, pp. 153–156, 2015.
- [27] G. G. Tang, J. R. Sun, W. Chen, H. Tang, Y. J. Wang, and C. S. Li, "Surfactant-assisted hydrothermal synthesis and tribological properties of flower-like MoS<sub>2</sub> nanostructures," *Micro and Nano Letters*, vol. 8, no. 3, pp. 164–168, 2013.
- [28] Y. M. Shi, H. N. Li, J. I. Wong et al., "MoS<sub>2</sub> surface structure tailoring via carbonaceous promoter," *Scientific Reports*, vol. 5, Article ID 10378, 2015.
- [29] S. Jiang, X. Yin, J. Zhang, X. Zhu, J. Li, and M. He, "Vertical ultrathin MoS<sub>2</sub> nanosheets on a flexible substrate as an efficient counter electrode for dye-sensitized solar cells," *Nanoscale*, vol. 7, no. 23, pp. 10459–10464, 2015.
- [30] J. Qian, Z. Peng, P. Wang, and X. Fu, "Bulk fabrication of WS<sub>2</sub> nanoplates: investigation on the morphology evolution and electrochemical performance," *ACS Applied Materials and Interfaces*, vol. 8, no. 26, pp. 16876–16884, 2016.
- [31] C. Lee, H. Yan, L. E. Brus, T. F. Heinz, J. Hone, and S. Ryu, "Anomalous lattice vibrations of single- and few-layer MoS<sub>2</sub>," *ACS Nano*, vol. 4, no. 5, pp. 2695–2700, 2010.
- [32] Y. Yu, C. Li, Y. Liu, L. Su, Y. Zhang, and L. Cao, "Controlled scalable synthesis of uniform, high-quality monolayer and few-layer MoS<sub>2</sub> films," *Scientific Reports*, vol. 3, no. 5, article 1866, 2013.
- [33] M. Xu, T. Liang, M. Shi, and H. Chen, "Graphene-like two-dimensional materials," *Chemical Reviews*, vol. 113, no. 5, pp. 3766–3798, 2013.
- [34] K. Kalantar-zadeh, J. Z. Ou, T. Daeneke, A. Mitchell, T. Sasaki, and M. S. Fuhrer, "Two dimensional and layered transition metal oxides," *Applied Materials Today*, vol. 5, pp. 73–89, 2016.



